Appendix for "Ballots and burials: Electoral turnovers and the health costs of elections during emergencies"

Table of Contents

A Additional information **2**

A.1 Municipal elections in France 4

A.2 Excess mortality estimation 5

A.3 Summary and balance statistics 6

A.4 Additional information on conditional-on-observables 7

B Extensions **9**

B.1 Change in council membership 9

B.2 Ideology as an alternative explanation 10

B.3 Higher vulnerability among left-leaning municipalities 14

B.4 Subsample with information on council resolution 18

C Robustness checks **19**

C.1 Robustness of conditional-on-observables strategy 19

C.2 Robustness of RD design 25

D Country-level panel dataset **28**

A Additional information

Figure A1: Death toll from Covid-19 in France over time

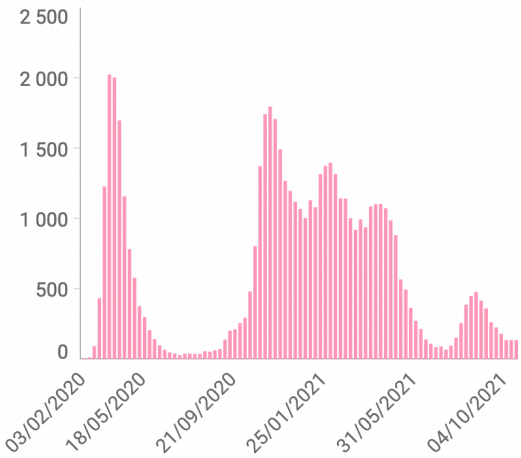

Note: Figure showing the number of deaths in France where the death certificate mentions Covid-19 over time. Source: https://www.santepubliquefrance.fr/dossiers/coronavirus-covid-19/coronavirus-chiffres-cles-et-evolution-de-la-covid-19-en-france-et-dans-le-monde.

Figure A2: Geographical variation in Covid-19 incidence in France

Note: The figure shows the all-age Covid-19 incidence rates at the municipality level for the week of 1–7 Feb 2021. During this week, rates varied between under 10 per 100,000 (yellow shading) to over 1,000 per 100,000 (dark blue shading). Variation over time can be seen at https://geodes.santepubliquefrance.fr/#c=indicator&f=0&i=sg_iris_imp.ti&s=2021-02-01-2021-02-07&t=a01&view=map10.

Figure A3: Nightlight emissions and their change 2014–2019

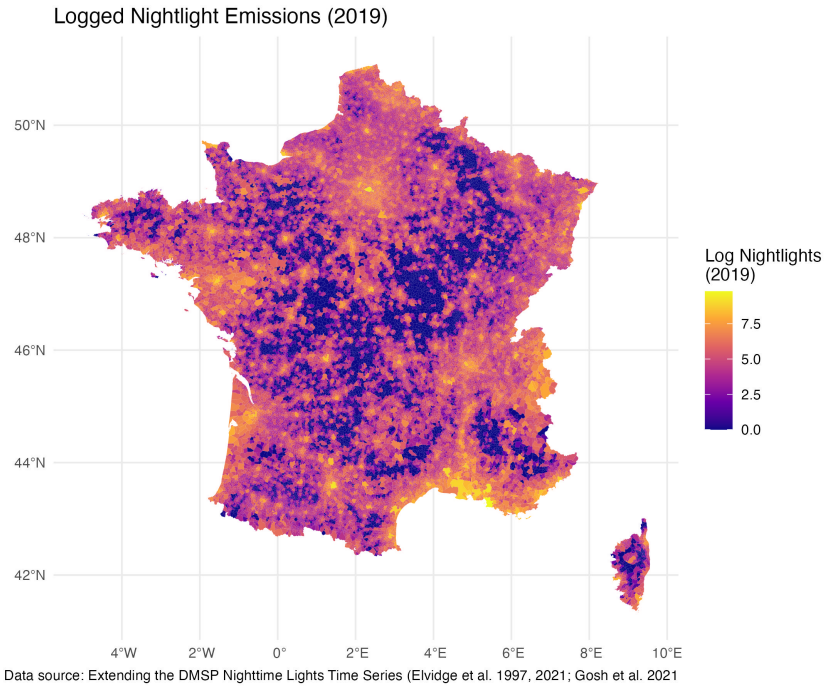

(a) (Logged) nightlight emissions 2019

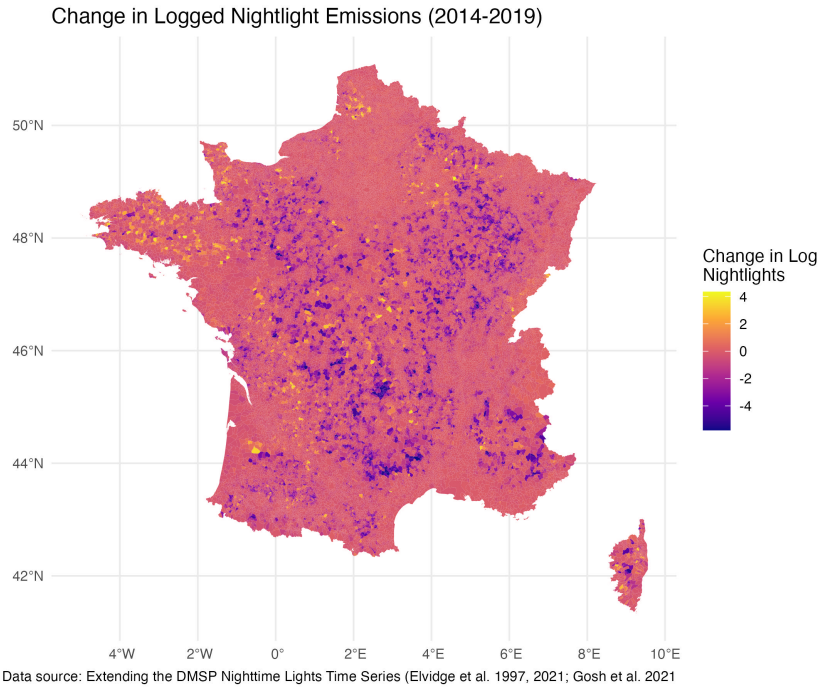

(b) Change in (logged) nightlight emissions 2014–19

Note: (Logged) nightlight emissions, measured with the DMSP Operational Linescan System (Elvidge et al. 1997; Elvidge et al. 2021), extension of series to 2019 provided by Ghosh et al. (2021).

A.1 Municipal elections in France

The municipal elections serve to choose the mayors of all of the nearly 35,000 municipalities in the country. Municipal elections in France are held every six years and, depending on the size of the municipality, consist of one or up to two rounds. In small municipalities with under 1,000 inhabitants, voters choose lists of candidates and are allowed to cast a vote for more than a single candidate in a majoritarian system. These are therefore not part of our sample, In larger towns and cities with more than 1,000 inhabitants, elections consist of one or two rounds. In the first round, all lists of candidates standing for the election compete against each other. In case no list obtains more than 50% of the vote, a run-off election is held in which all the lists that obtained more than 10% of the votes compete again for election.

This second round is usually held two weeks after the first round. In 2020 the first round of the municipal elections was held as scheduled on 15 March 2020, despite a partial lockdown in some places. However, as the number of cases of Covid-19 continued to increase, the day after the first round of the elections, President Macron announced that the second round would be postponed to an unspecified date, which was later set to June 28, 2020. Compared to the previous local elections in 2014, turnout dropped substantially. While in 2014, 63.5% of eligible voters went to cast their ballot in the first round of the elections, on March 15, 2020 less than half of eligible voters (44.7 percent) went to vote. This drop in participation was likely due to the circulation of the virus, as confirmed by a recent study (Noury et al. 2021).

Table A1: Political Affiliation of electoral lists in French municipal elections

Classification	**Name of the List**	**2014**	**2020**
extreme left	Extrême gauche	EXG	EXG
left	Front de gauche	FG	
left	Parti de gauche	PG	
left	Parti communiste français	COM	COM
left	France insoumise		FI
left	Parti socialiste	SOC	SOC
left	Union de la gauche	UG	UG
left	Parti radical de gauche		RDG
left	Divers gauche	DVG	DVG
left	Europe-Ecologie-Les Verts	VEC	VEC
diverse	Autre écologiste		ECO
diverse	Divers	DIV	DIV
diverse	Régionalistes		REG
diverse	Gilets jaunes		GJ
centre	La République en marche		REM
centre	Modem	MDM	MDM
centre	Union du centre	UC	UC
centre	Union des démocrates et indépendants	UDI	UDI
centre	Divers centre		DVC
right	Les Républicains	UMP	LR
right	Union de la droite	UD	UD
right	Divers droite	DVD	DVD
right	Debout la France		DLF
extreme right	Rassemblement national	FN	RN
extreme right	Extrême droite	EXD	EXD

Paris, Marseille, and Lyon differ from this voting rule as their population elects both representatives at the district level and city council members. The number of council members elected by each district depends on the relative population sizes. However, the mortality data is at the city level. We, therefore, excluded these cities from the sample.

Data on the on the first round of the 2020 elections can be found at https://www.data.gouv.fr/fr/datasets/elections-municipales-2020-resultats/ (accessed June 10, 2020); and for the second round at https://www.data.gouv.fr/fr/datasets/municipales-2020-resultats-2nd-tour/ (accessed July 1, 2020).

A.2 Excess mortality estimation

To estimate excess mortality during the Covid-19 pandemic, we use a type of Poisson regression model with municipality-specific baseline mortality rate before the pandemic and municipality-specific excess mortality factor during the pandemic:

$$\begin{aligned} N_{i,y} &\sim Poisson(\text{Pop}_{i,y}\lambda_{i,y}) \\ \log \lambda_{i,y} &= \log \lambda_i + \log mort_i \delta_{\text{covid year}}(y) \end{aligned}$$

where $N_{i,y}$ is the number of deaths observed in municipality i on the time period y (periods of 12 months starting from July 2015 to June 2019 and July 2020 to June 2021), $\text{Pop}_{i,y}$ is the population of municipality i during the time period y, λ_i is the baseline mortality rate of municipality i pre-covid (period July 2015—June 2019), $mort_i$, appearing in Eq. 1 is the excess mortality factor during the Covid-19 pandemic and $\delta_{\text{covid year}}(y)$ is an indicator function which takes value 0 for the period pre-covid and 1 for the period during the Covid-19 pandemic.

Because the number of municipalities is quite large (≈ 5000), and since the goal of this analysis is to obtain point estimates for the municipality-level excess mortality factor, we resort to Variational Inference, which is known for good performance in obtaining point estimates for a posterior distribution (Blei, Kucukelbir, and McAuliffe 2017). We use a stochastic variational inference algorithm (Kucukelbir et al. 2015) through the interface available in Stan (Stan Development Team and Stan Developement Team 2015).

We use vaguely informative priors on all parameters. To stabilize our estimation and regularize the baseline mortality estimation in small municipalities, we use a shrinkage-inducing prior on λ_i. However, we do not wish to shrink excess mortality estimates together, so we use independent priors for the $mort_i$ parameters:

$$\begin{aligned} \log \lambda_i &\sim \mathcal{N}(\mu_\lambda, \sigma_\lambda) \\ \mu_\lambda &\sim \mathcal{N}(0, 10) \\ \sigma_\lambda &\sim \mathcal{N}^+(0, 10) \\ \log mort_i &\sim \mathcal{N}(0, 10) \end{aligned}$$

A summary of the estimated parameters is provided in Table A2.

A.3 Summary and balance statistics

Table A2: Summary statistics

	mean	sd	min	max	count
Male/female ratio	0.96	0.09	0.67	2.57	4,912
Share over 65	0.21	0.07	0.04	0.52	4,912
Share over 75	0.10	0.04	0.01	0.31	4,912
Share over 80	0.06	0.03	0.01	0.23	4,912
Share immigrants	0.06	0.05	0.00	0.50	4,912
Share blue collar	0.11	0.04	0.01	0.29	4,912
Unemployment rate	0.12	0.05	0.02	0.40	4,912
Std of living in 10k	2.19	0.33	1.33	4.50	4,912
Pop density in 100/km2	5.20	12.76	0.05	195.97	4,912
Nightlight emissions 2019	5.54	1.14	0.00	9.34	4,912
Change in nightlight emissions	-0.21	0.50	-5.55	3.72	4,912
Change in share immigrants	0.02	0.02	-0.10	0.23	4,912
Change in unemployment rate	0.05	0.03	-0.01	0.25	4,912
Change in standard of living	-18.97	2.92	-38.33	-11.69	4,912
Number of candidates	2.03	1.31	1.00	14.00	4,912
Baseline mortality	$6.73e^{-3}$	$9.38e^{-3}$	$3.88e^{-4}$	$1.67e^{-1}$	4,912
Excess mortality 07/2020-06/2021	1.07	$5.28e^{-1}$	$2.85e^{-3}$	6.25	4,912
Mask-wearing mandate	0.43	0.50	0.00	1.00	4,912

Table A3: Balance after matching

	No turnover			Turnover			
	n	mean	sd	n	mean	sd	Diff
Male/female ratio	683	0.947	0.082	683	0.947	0.079	0.000
Share over 65	683	0.214	0.071	683	0.215	0.071	0.001
Share over 75	683	0.102	0.045	683	0.103	0.045	0.000
Share over 80	683	0.067	0.034	683	0.067	0.034	0.000
Share immigrants	683	0.060	0.056	683	0.064	0.058	0.004
Share blue collar	683	0.107	0.037	683	0.106	0.037	-0.001
Unemployment rate	683	0.121	0.044	683	0.122	0.045	0.001
Median standard of living in 10k	683	2.188	0.353	683	2.189	0.357	0.000
Pop density in 100/km2 (logged)	683	4.939	9.481	683	5.678	12.390	0.739
Nightlight emissions 2019	683	5.594	1.277	683	5.676	1.070	0.082
Change in nightlight emissions	683	-0.204	0.565	683	-0.203	0.429	0.002
Change in share immigrants	683	0.022	0.020	683	0.023	0.022	0.001
Change in unempl rate 2014-2020	683	0.053	0.028	683	0.053	0.027	0.001
Change in standard of living	683	-18.989	3.090	683	-18.975	3.084	0.014
Number of candidates	683	2.792	1.279	683	2.840	1.270	0.048
Baseline mortality	683	0.007	0.009	683	0.007	0.009	0.000
Excess mortality 07/2020-06/2021	683	1.035	0.500	683	1.132	0.528	0.097**

* $p < 0.05$, ** $p < 0.01$.

A.4 Additional information on conditional-on-observables

Municipalities where incumbents win likely differ from those where challengers gain power. For example, winning incumbents are likely helped by favorable local economic development, whether or not they contributed to it. Economic development, in turn, is likely correlated with better health outcomes, possibly because higher incomes alleviate stresses caused by poverty (Banerjee and Duflo 2011; Pryor et al. 2019; Schaub 2021), or because economic growth frees resources for funding local medical services (Wagstaff 2002). To systematically trace this and other confounders, we derived a directed acyclic graph (DAG), pictured in Figure A4. The DAG makes explicit the causal relationships between our dependent variable (excess mortality), our independent variable (electoral turnovers), and potential confounders (Elwert 2014). Apart from poverty, which we measure in terms of unemployment rates, median income, and nightlight emission, confounders include employment in basic service and blue-collar jobs (which increased exposure to Covid-19 and hence the risk of deadly courses of disease; cp. Patel et al. 2020), the share of the foreign population (which was associated with various risk factors; cp. Williamson et al. (2020)), and the male-to-female ratio. We also control for the changes in these variables between 2014 and 2019/20. Probably the most

Figure A4: Directed acyclic graph detailing the relationship between electoral transitions and excess mortality

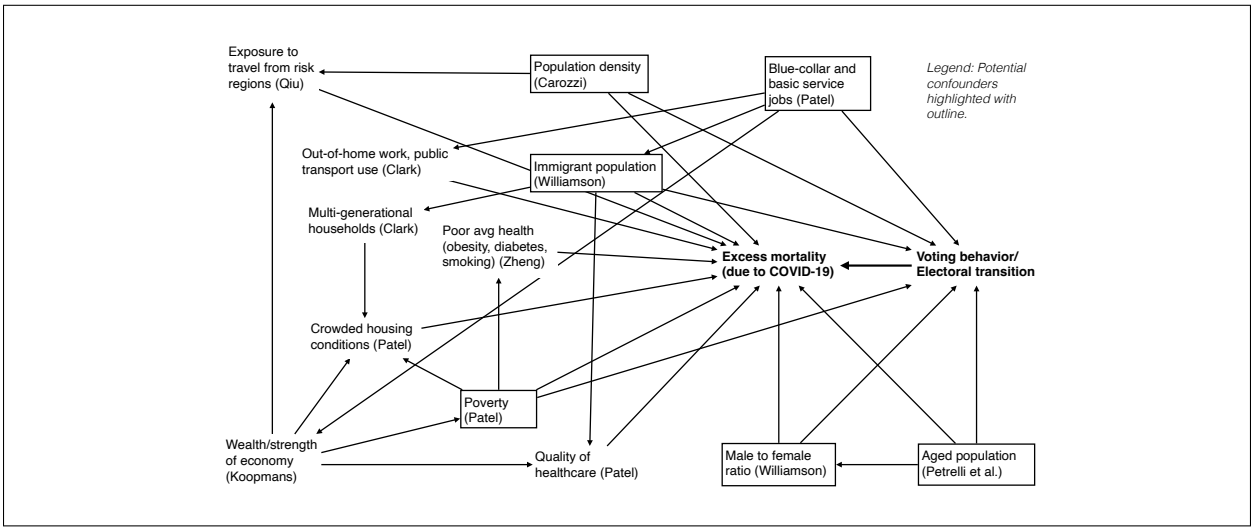

important confounders are age and urbanity. Both of these factors were prominent among the causes of higher mortality rates due to Covid-19. A study by Petrilli et al. (2020) showed that in the United States, mortality after diagnosis with Covid-19 was 200 times higher for those older than 70 than for those younger than 40. At the same time, age and urban residence are also classic predictors of voting behavior (Campbell et al. 1960). Other factors, such as crowded housing, poorer health among the less affluent, or the frequency of working outside the home, were also important predictors of Covid-19 infection and are to some extent determinants of voting behavior. However, these clearly lie on the causal path from poverty and social class to excess mortality and should therefore not be considered confounders.

Table A4: Effect of electoral turnover on excess mortality

	(1)	(2)	(3)	(4)	(5)	(6)	(7)
Electoral turnover (incumbent	0.073**	0.080**	0.077**	0.096**	0.022		0.167**
lost office in 2020)	(0.021)	(0.023)	(0.023)	(0.027)	(0.032)		(0.053)
Turnover × vote share					0.002*		
for left-leaning parties					(0.001)		
Share of council membership						-0.017	0.113†
remaining in place						(0.051)	(0.062)
Turnover × share							-0.282
council remaining in place							(0.174)
Vote share for left-leaning					0.000		
parties					(0.000)		
Male-to-female ratio (logged)		-0.070	-0.086	-0.124	-0.083	-0.089	-0.081
		(0.096)	(0.097)	(0.197)	(0.097)	(0.098)	(0.097)
Share immigrants (logged)		0.015	0.040*	-0.002	0.040*	0.041**	0.040*
		(0.013)	(0.016)	(0.024)	(0.016)	(0.016)	(0.016)
Share blue collar (logged)		-0.034	0.005	-0.126*	0.007	0.008	0.004
		(0.027)	(0.034)	(0.052)	(0.034)	(0.034)	(0.034)
Population density		-0.020	-0.038	-0.106	-0.043	-0.031	-0.040
		(0.045)	(0.052)	(0.095)	(0.052)	(0.052)	(0.052)
Pop density, 2nd polynom		0.005	0.006	0.011	0.006	0.005	0.006
(logged)		(0.004)	(0.005)	(0.008)	(0.005)	(0.005)	(0.005)
Share over 65 (logged)		2.446*	1.762	1.523	1.771†	1.736	1.670
		(1.028)	(1.073)	(1.881)	(1.072)	(1.077)	(1.076)
Share over 75 (logged)		-0.986	-1.456	-14.794	-1.755	-0.650	-1.223
		(4.830)	(4.954)	(9.308)	(4.950)	(4.967)	(4.965)
Share over 80 (logged)		14.476*	14.960*	31.448**	15.288*	13.920*	14.911*
		(6.385)	(6.498)	(11.852)	(6.493)	(6.516)	(6.513)
Share over 65x75 (logged)		-8.877	-0.369	47.786	1.265	-3.368	-0.471
		(19.064)	(19.519)	(36.200)	(19.508)	(19.571)	(19.565)
Share over 65x80 (logged)		-27.976	-29.664	-116.802†	-31.592	-24.774	-29.005
		(35.126)	(35.557)	(63.884)	(35.533)	(35.653)	(35.626)
Share over 75x80 (logged)		-44.547†	-49.054†	-4.718	-48.509†	-50.250†	-51.599†
		(26.814)	(27.593)	(48.900)	(27.568)	(27.707)	(27.681)
Share over 65x75x80 (logged)		134.930*	123.868†	110.291	122.507†	125.338†	127.631†
		(65.119)	(66.747)	(105.300)	(66.684)	(67.031)	(66.974)
Std of living in 10k (logged)		-0.051	-0.012	-0.169	0.007	-0.002	-0.008
		(0.097)	(0.116)	(0.178)	(0.116)	(0.117)	(0.117)
Baseline mortality (logged)		-4.416**	-4.461**	-7.688**	-4.369**	-4.494**	-4.357**
		(1.053)	(1.065)	(2.276)	(1.065)	(1.071)	(1.070)
Share unemployed (logged)		0.137*	0.085	0.206†	0.074	0.087	0.085
		(0.056)	(0.062)	(0.108)	(0.062)	(0.062)	(0.062)
Change in share immigrants		-0.222	-0.199	-0.349	-0.192	-0.195	-0.165
		(0.557)	(0.582)	(1.062)	(0.581)	(0.585)	(0.584)
Change in unempl rate		-1.419*	-1.234†	-2.443†	-1.188†	-1.304†	-1.232†
2014-2020		(0.688)	(0.718)	(1.353)	(0.718)	(0.721)	(0.721)
Change in (logged) median		0.277	-0.070	-0.539	-0.001	-0.099	-0.091
income		(0.363)	(0.401)	(0.687)	(0.401)	(0.403)	(0.403)
Nightlight emissions 2019		0.043**	0.038**	0.059**	0.037**	0.035**	0.037**
		(0.009)	(0.010)	(0.018)	(0.010)	(0.010)	(0.010)
Change in nightlight emissions		-0.037*	-0.037†	-0.018	-0.036†	-0.033†	-0.036†
		(0.018)	(0.019)	(0.033)	(0.019)	(0.019)	(0.019)
Constant	1.059**	1.211	0.587	-0.195	0.712	0.534	0.488
	(0.008)	(0.832)	(0.915)	(1.558)	(0.915)	(0.919)	(0.918)
Pretreatment controls	Yes	Yes	Yes	Yes	Yes	Yes	Yes
Départements FEs	No	No	Yes	No	Yes	Yes	Yes
N	4,912	4,912	4,912	1,366	4,912	4,885	4,885
R2	0.00	0.04	0.07	0.06	0.07	0.07	0.07

Note: Full results for Table 1 in main text. OLS estimates, † $p < 0.1$, * $p < 0.05$, ** $p < 0.01$.

In our models, we account for the identified confounders by controlling for control for the prevalence of blue-collar and service jobs with the share of such jobs in the local industry, for the presence of immigrants with the share of foreigners, and for poverty with local GDP.

We therefore flexibly control for age by including three variables (share older than 65, older than 75, and older than 90) and their interactions and for population density by including its linear and square terms. We log-transform each of these variables to account for the presence of clear outliers. We also include a categorical variable for the number of candidates running in an electoral race because winning margins tend to be systematically smaller for races with a larger number of candidates.

B Extensions

B.1 Change in council membership

The municipal elections in France appoint simultaneously the mayors and the city councils. This fact allows us to investigate whether disruptions in the entire elected team are associated with similar negative effects as disruptions in the leader. To investigate this idea, we retrieved information on the names of the previous municipal councilors (in office from 2014-2020) and compared them with the names of the newly appointed councilors (from 2020 onward). From this information, we calculated the percentage of council members who retained their seats, which we use as an alternative independent variable in our analysis. We should start by noting that there is, of course, an overlap between mayoral turnover and the degree to which councils changed. On average, in municipalities where the mayor won another term, 49% of council members stayed in office, while in municipalities where the mayor lost, only 24% of council members stayed in office—although there is considerable variation in this figure that we can exploit for our analysis.

As a first step, we examine whether there is an effect of the proportion of council members that changed on excess mortality. However, as shown in Table 1, Model 6 in the main text, this is not the case—the coefficient is small and statistically insignificant. That is, legislative instability alone does not correlate with higher excess mortality in the short term. As a second step, we therefore test the idea that it is the combination of a change in the top leadership (the mayor) and a change in council membership that is unfavorable for population health. We do so by interacting the indicator for turnover with the proportion of council members replaced in the same election. The results are presented in Figure A5, which shows the marginal effects of electoral turnover conditional on the degree to which council membership remained stable. We see that the effect of turnover is more severe the smaller the proportion of council members who remain in office—to the extent that in municipalities where around 35% of the council members remained in place, the effect

Figure A5: Interaction with change in municipal council membership

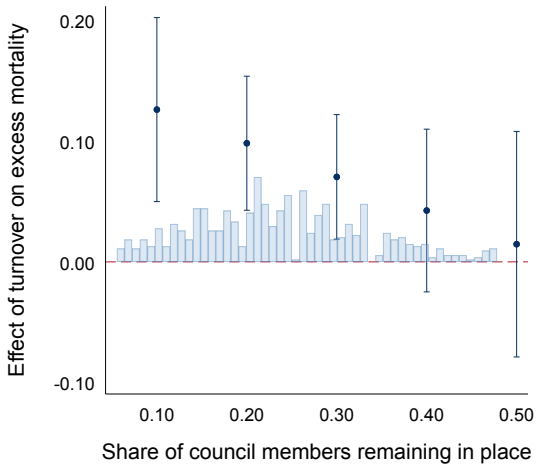

Note: Effect of electoral turnovers on excess mortality conditional on the share of council members staying on after the election. Marginal effects after OLS regression. Markers are point estimates, lines 95% confidence intervals. The histogram in the background shows the density distribution of the share of council members remaining in office in municipalities that experienced a turnover.

of electoral turnover becomes indistinguishable from zero.

On the one hand, it is important not to overstate the importance of this result. As can be seen from the histogram in the background, which shows the density distribution of the proportion of councilors remaining in office in municipalities with turnovers, in the vast majority of municipalities, turnover is still associated with an increased level of excess mortality. Nevertheless, the analysis clearly supports the idea that it is the change in the political leadership that matters—but only in cases where the top executive position also changes hands. We take this finding as support for the idea that it is indeed disruption—which is higher when more council members leave along with the mayor—that drives excess mortality in the context of electoral turnovers.

B.2 Ideology as an alternative explanation

A plausible alternative explanation for our results relates to the political ideology of newly elected mayors and its effect on health. As discussed in the theory section, previous work has shown that left-wing politicians tend to improve health outcomes in the long run, for example by expanding welfare and public health programs, while right-wing politicians tend to undermine these outcomes through austerity measures and program cuts.

Since newly elected right-wing mayors will thus tend to be less supportive of public welfare spending than previous mayors, electoral turnover could lead to (short-term) increases in local mortality. If turnovers occurred on a large scale, changes in ideological orientation could even lead to a large-scale deterioration in health outcomes. This would be the case, for example, if the majority of incumbent mayors were left-wing and the majority of challengers with the highest chances of winning were right-wing. In such a situation, we might find that electoral turnovers, on average, lead to increased mortality. In this case, the effect of turnovers would depend not on the disruption associated with a transition of power, but rather on the political ideology of the newly elected candidates, who would de-prioritize spending on public welfare programs.

To investigate whether this dynamic could explain the patterns presented above, we first consider the ideology of newly elected mayors. If incumbent mayors were predominantly left-wing and their main challengers disproportionately right-wing, elections could systematically shift power toward right-wing candidates—even in close races. Such a shift, in turn, could explain the increased excess mortality in municipalities with electoral turnover. We test for this idea as best as we can with the available data.

Unfortunately, the analysis of ideological leanings is limited by a legislative change between the two previous rounds of local elections. As mentioned above, in 2014, all candidates from municipalities with more than 1,000 inhabitants were

Figure A6: Political orientation of winning candidate by turnover

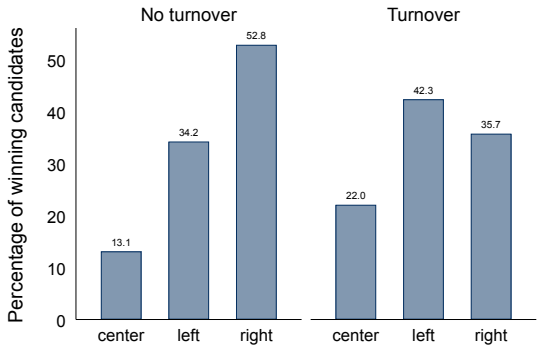

Note: Political affiliation of winning candidates in municipalities with and without turnover. Figure based on ideological orientation of the 1,494 municipalities with more than 3,500 inhabitants.

classified by the French Ministry of the Interior according to their political affiliation, meaning that we can classify all 4,952 incumbents along the left-center-right dimension. For the 2020 elections, however, the reporting threshold was moved up to 3,500 inhabitants, which means that we do not know the affiliation of candidates from smaller municipalities. Moreover, 182 candidates were classified as "other" (*divers*), meaning that we cannot infer their affiliation, leaving us with a reduced sample of 1,494 observations from larger municipalities.

Keeping this limitation in mind, in Figure A6 we plot the ideological orientation of winning candidates in races without and with turnovers, i.e., where incumbents held on to power or lost. In order for right-wing ideology to be a plausible explanation driving our findings, we should see their share increase among newly elected mayors. However, as shown, newly elected mayors were clearly *less* likely to belong to the political right than incumbent mayors. In other words, instead of a right-shift, there appears to have been a marked shift towards the political center and left. This result is in line with French media reports on the topic that also noted reduced support for right-wing political parties during the 2020 elections (e.g., Le Monde 2020), and holds up in a regression analysis controlling for our standard set of covariates, as shown in Table A6 below.

While the apparent swing away from the political right makes it unlikely that our overall results are driven by ideology, we also conduct a second test. Specifically, we use the regression discontinuity setup to directly test the implication of an ideology-based explanation that left-wing victories are associated with lower excess mortality. For this test, we code a new forcing variable: the "left winning margin." This variable considers only electoral races where a left-wing incumbent or left-wing challenger took part, and takes values corresponding to their margin of victory or defeat. Positive values correspond to left-wing candidate wins, negative values to left-wing candidate losses.

The results are presented in Table A5. In stark contrast to what we might expect from an ideology-based explanation, marginal wins by left-wing candidates are associated with significantly *higher* excess mortality (Models 1–3). Why this is so can be seen by further

Table A5: Effect of close left-wing candidate win (RD estimates)

	All			Incumbents			Challengers		
	(1) Convent	(2) Bias-corr	(3) Robust	(4) Convent	(5) Bias-corr	(6) Robust	(7) Convent	(8) Bias-corr	(9) Robust
Effect of marginal left-wing candidate win	0.259*	0.308*	0.308*	-0.196	-0.235†	-0.235	0.525**	0.533**	0.533**
	(0.128)	(0.128)	(0.149)	(0.122)	(0.122)	(0.150)	(0.180)	(0.180)	(0.193)
Pretreatment controls	Yes	Yes	Yes	Yes	Yes	Yes	Yes	Yes	Yes
Candidate FEs	Yes	Yes	Yes	Yes	Yes	Yes	Yes	Yes	Yes
N	830	830	830	394	394	394	436	436	436
Bandwidth	20.06	33.70	33.70	9.79	14.99	14.99	11.03	14.32	14.32

Note: Regression discontinuity results. Effect of left-wing candidate incumbent marginally winning their election on excess mortality for all candidates (Models 1–3), left-wing incumbents (Models 4–6), and left-wing challengers (Models 7–9). Estimation method (conventional, bias-corrected, robust, see: Calonico, Cattaneo, and Titiunik 2014; Calonico et al. 2019) indicated above the estimates; p-values in parentheses, † $p < 0.1$, * $p < 0.05$, ** $p < 0.01$.

splitting the sample into wins by left-wing incumbents versus left-wing challengers. For incumbent wins (Models 4–6), we see a (marginally statistically significant) *negative* effect on excess mortality. Left-wing *challenger* wins following an electoral turnover from center or right-wing incumbents are instead associated with substantially large and statistically significant increases in excess mortality (Models 7–9). Estimates for mask mandates are analogous, with left-wing incumbent wins being associated with a higher likelihood of a mandate, and left-wing challenger wins associated with fewer mandates, as shown in Table A8 below. The results are also confirmed in a similar test, where the investigate the effect of turnovers on excess mortality depending on the ideological leaning of the winner using our OLS regression setup. In addition, in Table A7 we check for evidence of ideological sorting at the threshold, i.e., whether candidates of a certain political orientation are more likely to win marginal elections. Reassuringly, we find no evidence of this.

The observed patterns are therefore fully consistent with our core results, where incumbent wins are associated with lower excess mortality and turnovers are associated with higher excess mortality. Thus, despite the logical appeal of an ideology-based explanation, there is no evidence that this explanation can account for our results. Instead, the evidence in this section suggests that it is in fact the turnovers themselves and the associated disruptions that are responsible for the increase in excess mortality.

Relative electoral gains of candidates of different ideological orientations

Figure A6 above suggests that in the municipal elections there was a relative move away from the political right towards the political center. Table A6 shows that this relationship also holds in a regression including the full set of controls. As the ideological orientation of winning candidates was only recorded for municipalities of 3,500 inhabitants or more, we work with a reduced sample of 1,494 municipalities.

Table A6: Political affiliation of winner

	Political affiliation of winner		
	(1)	(2)	(3)
	Center	Left	Right
Electoral turnover	0.065*	0.143**	-0.208**
	(0.028)	(0.034)	(0.037)
Pretreatment controls	Yes	Yes	Yes
Départements FEs	Yes	Yes	Yes
N	1,494	1,494	1,494
R2	0.11	0.26	0.23

† $p < 0.1$, * $p < 0.05$, ** $p < 0.01$.

Potential sorting at threshold by ideology

This analysis tests whether there was sorting at the threshold by ideology, i.e., whether in close elections, candidates of a specific political leaning (center, left, or right) were more likely to emerge victorious. This would be problematic because it would violate the local randomization assumption at the threshold. It would also challenge our claim that the higher excess mortality rates in areas with an electoral turnover are really due to the change in government, and not a consequence of an ideological shift. We therefore repeat our main

RDD specification using the indicators for center-, left-, or right-affiliation of the winner as dependent variables. As above, we have to work with the reduced sample. Reassuringly, the results of this test, presented in TableA7, do not suggest that there was any sorting at the threshold. All RDD estimates are close to zero and statistically insignificant. In other words, candidates of all ideological affiliations were similarly likely to win an election.

Table A7: Testing for RDD effect on political affiliation of winner

	Winner center			Winner left-wing			Winner right-wing		
	(1) Convent	(2) Bias-corr	(3) Robust	(4) Convent	(5) Bias-corr	(6) Robust	(7) Convent	(8) Bias-corr	(9) Robust
Effect of marginal incumbent win	-0.017 (0.084)	0.006 (0.084)	0.006 (0.098)	0.022 (0.107)	0.040 (0.107)	0.040 (0.128)	-0.025 (0.107)	-0.055 (0.107)	-0.055 (0.126)
Pretreatment controls	Yes	Yes	Yes	Yes	Yes	Yes	Yes	Yes	Yes
N	1,494	1,494	1,494	1,494	1,494	1,494	1,494	1,494	1,494
Bandwidth	11.70	18.70	18.70	13.02	18.70	18.70	10.21	16.71	16.71

Note: Regression discontinuity results. Effect of marginal election wins on the probability of a candidate from the political center, left, and right being elected mayor. Estimation method (conventional, bias-corrected, robust, see: Calonico, Cattaneo, and Titiunik 2014; Calonico et al. 2019) indicated above the estimates; p-values in parentheses, † $p < 0.1$, * $p < 0.05$, ** $p < 0.01$.

RD results for mask mandate with left margin as forcing variable

Table A8: Effect of close left-wing candidate win on mask mandate (RD estimates)

	All			Incumbents			Challengers		
	(1) Convent	(2) Bias-corr	(3) Robust	(4) Convent	(5) Bias-corr	(6) Robust	(7) Convent	(8) Bias-corr	(9) Robust
Effect of marginal left-wing candidate win	0.062** (0.016)	0.039* (0.016)	0.039 (0.024)	0.092** (0.001)	0.087** (0.001)	0.087** (0.018)	-0.097** (0.008)	-0.124** (0.008)	-0.124** (0.043)
Pretreatment controls	Yes	Yes	Yes	Yes	Yes	Yes	Yes	Yes	Yes
N	830	830	830	394	394	394	436	436	436
Bandwidth	10.25	16.19	16.19	7.31	11.27	11.27	5.97	9.32	9.32

Note: Regression discontinuity estimates for marginal incumbent wins on the likelihood of having implemented a mask mandate, using data on all left-wing candidates (Models 1–3), left-wing incumbents (Models 4–6), and left-wing challengers (Models 7–9). Estimation method (conventional, bias-corrected, robust, see: Calonico, Cattaneo, and Titiunik 2014; Calonico et al. 2019) indicated above the estimates; p-values in parentheses, † $p < 0.1$, * $p < 0.05$, ** $p < 0.01$.

Effect on excess mortality by ideological affiliation of the winner

As an alternative way of probing for the potential role of ideology, we estimated the effect on excess mortality of the interaction between the indicator for electoral turnovers and the ideological affiliation of the winner of the election winner. We then calculated the marginal effect of turnovers for each of the three possible ideological leanings. Results for this analysis are presented in Table A9, and the original interaction models can be found in Table A10.

We first present overall results (Models 1-3), then restrict our sample to left-leaning municipalities (Models 4-6), and then to municipalities where an explicitly left-wing incumbent contested the election (Models 7-9). We see that in all but the last scenario, turnovers to left-leaning candidates were associated with the largest (and statistically significant) *increases*

Table A9: Effect of electoral turnover on excess mortality depending on ideological leaning of winner

	All municipalities			Left-leaning municipalities			Municip. with left-wing incumbents		
	(1)	(2)	(3)	(4)	(5)	(6)	(7)	(8)	(9)
Ideol. leaning of winner:	Center	Left-wing	Right-wing	Center	Left-wing	Right-wing	Center	Left-wing	Right-wing
Electoral turnover	0.012	0.116**	-0.059	0.087	0.120**	-0.020	0.173	0.101	0.063
	(0.053)	(0.038)	(0.039)	(0.078)	(0.040)	(0.055)	(0.158)	(0.065)	(0.221)
Pretreatment controls	Yes	Yes	Yes	Yes	Yes	Yes	Yes	Yes	Yes
Départements FEs	Yes	Yes	Yes	Yes	Yes	Yes	Yes	Yes	Yes
N	1,494	1,494	1,494	1,009	1,009	1,009	521	521	521

Note: Effect of electoral turnover on excess mortality, depending on the ideological leaning of the winner for all municipalities (Models 1-3), left-leaning municipalities (Models 4-6), and municipalities with a left-wing incumbent (Models 7-9). Marginal effects after OLS regression, see Table A10 below for the interaction models, † $p < 0.1$, * $p < 0.05$, ** $p < 0.01$.

in excess mortality, while the least consequential type of turnover were turnovers to right-wing candidates. These results mirror those of the left-wing margin analysis (Table A5) in the main text, and provide further evidence against the—otherwise plausible—idea that the effect we observe is caused by right-wing challengers taking over the mayor's office.

Table A10: Effect of electoral turnover on excess mortality depending on ideological leaning of winner

	(1) All municip.	(2) Left-leaning	(3) Left-wing inc.
Left × Turnover (ref.)			
Center × Turnover	-0.104	-0.033	0.072
	(0.064)	(0.087)	(0.171)
Right × Turnover	-0.176**	-0.140*	-0.038
	(0.053)	(0.067)	(0.230)
Left (ref., const.)			
Center (const.)	0.037	0.041	0.138†
	(0.031)	(0.040)	(0.074)
Right (const.)	0.036†	0.053*	-0.024
	(0.022)	(0.026)	(0.211)
Turnover (const.)	0.116**	0.120**	0.101
	(0.038)	(0.040)	(0.065)
Pretreatment controls	Yes	Yes	Yes
Départements FEs	Yes	Yes	Yes
N	1,494	1,009	521

Note: Interaction models used in the calculation of marginal effects presented in Table A9 above. The abbreviation ref. stands for reference category, and const. for constitutive term. OLS estimates, † $p < 0.1$, * $p < 0.05$, ** $p < 0.01$.

B.3 Higher vulnerability among left-leaning municipalities

The tables and figure below provide support for the claim that left-leaning municipalities supported a higher population of vulnerable people, who then contributed to higher excess mortality following electoral turnovers. Table A11 regresses baseline mortality, that is, mortality during 2015 to 2019, on the political composition of municipal councils 2014 to 2020.

We can see that the vote share for left-leaning council members predicts a lower baseline mortality (Model 1), whereas the vote share for right-leaning members predicts a higher baseline mortality (Model 3). Excess mortality is then positively predicted by the vote share for left-leaning council members in 2014 (Model 4), but not by the vote share for center- or right-leaning council members ((Models 5 and 6)—replicating the findings from our main analysis.

Table A11: Association between mortality political affiliation of municipality

	Baseline mortality			Excess mortality		
	(1)	(2)	(3)	(4)	(5)	(6)
Vote share left-leaning parties 2014-2020	-0.089**			0.060*		
	(0.034)			(0.024)		
Vote share center parties 2014-2020		0.157			-0.047	
		(0.118)			(0.083)	
Vote share right-leaning parties 2014-2020			0.062†			-0.025
			(0.032)			(0.023)
Constant	-0.580	-0.509	-0.597	0.508	0.460	0.495
	(1.294)	(1.295)	(1.295)	(0.912)	(0.912)	(0.913)
Pretreatment controls	Yes	Yes	Yes	Yes	Yes	Yes
Départements FEs	Yes	Yes	Yes	Yes	Yes	Yes
N	4,912	4,912	4,912	4,912	4,912	4,912
R2	0.39	0.39	0.39	0.04	0.04	0.04

Note: Regression of excess and baseline mortality on the vote share obtained by left-, center-, and right-leaning parties. OLS regression, p-values in parentheses, † $p < 0.1$, * $p < 0.05$, ** $p < 0.01$.

Table A12a shows correlations between the vote share for left-leaning municipal council members and known risk factors predicting higher mortality as shown in Figure A4 above. We can see that votes shares for the political left are correlated in ways increasing mortality risk with all factors but the male-female share.

A similar picture arises when we correlate the vote share for left-leaning parties with health-related services (Table A12b). All services for which we could obtain data are positively and statistically significantly correlated withe the vote-share for left-wing parties, underlining the point that service provision is indeed higher here.

Figures A7a and Figures A7b illustrate this point graphically. The figures show the values for summary vulnerability and service-provision indices separately for left- vs. non-left-leaning municipalities. We calculated the indicators by standardizing and averaging over the different mortality risk factors and health service provision levels, respectively, and re-scaling to 0–100. We can see that both indices are significantly higher in left-leaning municipalities. Despite of the much higher mortality risks, and arguably due to the better services available, fewer people died in the pre-pandemic period in these vulnerable municipalities. Figures A7c and Figures A7d provide a historical comparison, using data from 2014 and 2016, respectively. We see that while vulnerability stayed largely constant over time, there was a general downward trend in health services in both centre-/right-leaning and left-leaning municipalities.

Table A12: Correlation with vote share for left-leaning parties

(a) Mortality risk factors

	Votes left	Share imm.	M. stnd. l.	Unempl.	Ov. 80
Left vote share 2014	1.00				
Share immigrants	0.05**	1.00			
Median standard of living in 10k	-0.23**	0.02	1.00		
Unemployment rate	0.22**	0.31**	-0.62**	1.00	
Share over 80	0.02	-0.08**	-0.34**	0.31**	1.00

(b) Health-related services

	Votes left	Em. serv.	Gen. pract.	Nurses	Pharm.
Left vote share 2014	1.00				
Emergency services p.c. (logged)	0.05**	1.00			
General practioners p.c. (logged)	0.12**	0.52**	1.00		
Nurses p.c. (logged)	0.14**	0.47**	0.80**	1.00	
Pharmacists p.c. (logged)	0.14**	0.58**	0.86**	0.81**	1.00

Note: Correlations of vote share for left-leaning municipal council members in 2014 (who got to sit in the council between 2014 and 2020) and a) known risk factors predicting higher mortality (cp. Figure A4 above), * $p < 0.05$.

Figure A7: Left-leaning vs. non-left-leaning municipalities

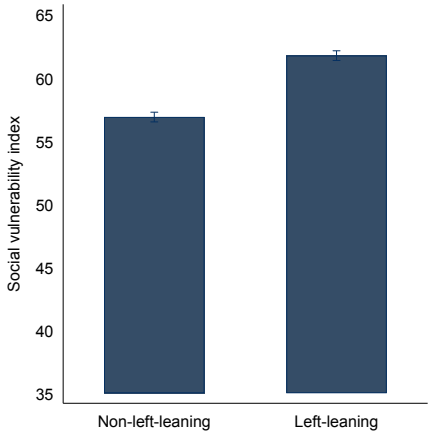

(a) Mortality risk index, 2020 data

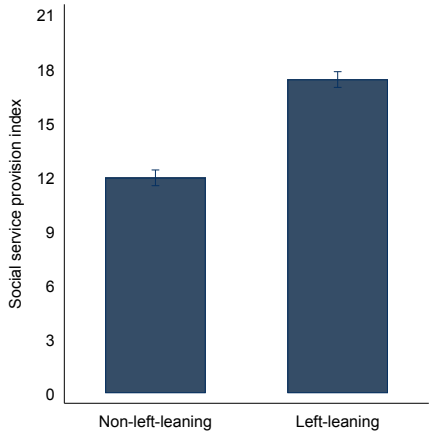

(b) Health-services index, 2020 data

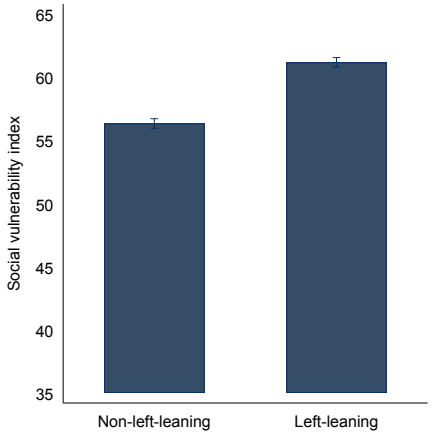

(c) Mortality risk index, 2014 data

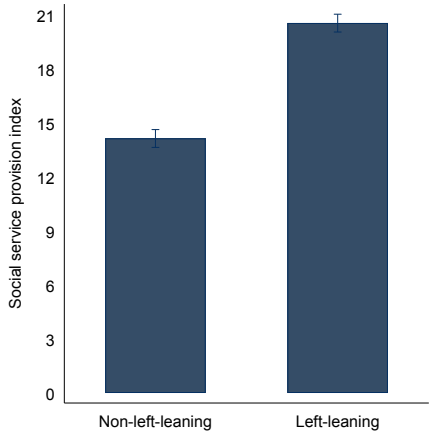

(d) Health-services index, 2016 data

B.4 Subsample with information on council resolution

Table A13: Balance for randomly drawn subsample of municipalities contacted to provide information on municipal council resolutions

	No turnover			Turnover			
	n	mean	sd	n	mean	sd	Diff
Male/female ratio	50	0.958	0.083	50	0.938	0.079	-0.020
Share over 65	50	0.218	0.072	50	0.212	0.057	-0.006
Share over 75	50	0.100	0.044	50	0.099	0.036	-0.001
Share over 80	50	0.065	0.033	50	0.064	0.026	-0.001
Share immigrants	50	0.054	0.051	50	0.063	0.055	0.010
Share blue collar	50	0.110	0.039	50	0.110	0.036	-0.000
Unemployment rate	50	0.116	0.052	50	0.129	0.041	0.013
Std of living in 10k	50	2.192	0.326	50	2.097	0.227	-0.095
Pop density in 100/km2	50	4.226	8.137	50	5.696	7.785	1.470
Number of candidates	50	2.620	0.987	50	3.040	1.498	0.420
Baseline mortality	50	0.004	0.007	50	0.003	0.004	-0.000

* $p < 0.05$, ** $p < 0.01$. *Note:* No statistically significant differences in Table.

Table A14: Balance for 52 municipalities that provided information on municipal council resolutions

	No turnover			Turnover			
	n	mean	sd	n	mean	sd	Diff
Male/female ratio	26	0.959	0.084	26	0.930	0.075	-0.029
Share over 65	26	0.205	0.062	26	0.213	0.058	0.008
Share over 75	26	0.097	0.038	26	0.103	0.038	0.007
Share over 80	26	0.062	0.029	26	0.068	0.028	0.005
Share immigrants	26	0.058	0.060	26	0.058	0.044	-0.000
Share blue collar	26	0.109	0.039	26	0.110	0.035	0.001
Unemployment rate	26	0.118	0.056	26	0.132	0.039	0.014
Std of living in 10k	26	2.219	0.371	26	2.088	0.204	-0.132
Pop density in 100/km2	26	4.864	10.745	26	6.717	9.258	1.853
Number of candidates	26	2.654	1.129	26	3.385	1.768	0.731
Baseline mortality	26	0.007	0.010	26	0.007	0.007	-0.000

* $p < 0.05$, ** $p < 0.01$. *Note:* No statistically significant differences in Table.

Table A15: Poisson and negative binomial regressions of count of municipal council resolutions mentioning Covid-19 on indicator for electoral turnover

	(1) Nr mentions Covid-19	(2)
Electoral turnover	-0.953**	-0.953
	(-4.21)	(-1.52)
Constant	0.990**	0.990†
	(8.29)	(2.30)
α		1.495**
		(4.83)
N	52	52

Note: The table shows the results of a Poisson (Model 1) and a negative binomial (Model 2) regression model of the number of municipal council resolutions (*arrêtés municipaux*) mentioning Covid-19 on the indicator for electoral turnover † $p < 0.1$, * $p < 0.05$, ** $p < 0.01$.

Table A16: Predictive margins for indicator for electoral turnover after Poisson and negative binomial regression

	(1) Nr mentions Covid-19	(2)
Elctoral turnover	1.038	1.038
	(5.20)	(2.19)
No turnover	2.692	2.692
	(8.37)	(2.32)
N	52	52

Note: The table shows predictive margins for the indicator for electoral turnover following the Poisson and negative binomial regressions presented in Table A15 † $p < 0.1$, * $p < 0.05$, ** $p < 0.01$.

C Robustness checks

C.1 Robustness of conditional-on-observables strategy

C.1.1 Vulnerability to omitted variable bias

First, using the approach suggested by Oster (2019), we estimate the relative amount of confounding that would be required to eliminate our treatment effect. The approach compares the coefficient estimate on turnover when no controls are included ($\beta_1 = 0.73$, see Table 1) with that when the full set of controls is included ($\beta_1 = 0.77$), and the corresponding R^2 values. Following Oster (2019), we then estimate δ, a measure of how much stronger the influence of the omitted variables would have to be (relative to the included covariates) to move our estimate to zero. Assuming a maximum feasible R^2 of 1.3 times the observed maximum R^2 in the model with all controls, as suggested by the author based on experimental baselines, we estimate $\delta = 18$. In other words, the influence of omitted variables would have to be 18 times as strong as the already included, fairly extensive set of controls—something

we consider highly unlikely. Our results, therefore, appear to be highly robust to omitted variable bias.

C.1.2 Different combinations of control variables

Next, we test how sensitive our main result—the effect of electoral turnovers on excess mortality—is to the inclusion or exclusion of control variables. We first consider an approach where all combinations of control variables would be equally valid, and examine what would have been our conclusion on the turnover effect had we chosen any specific combination. For this, we regress the outcome on all 2^k possible combinations of k control variables (omitting the empty set) using Equation 1. For the 20 included variables, this means running 1,048,576 separate regressions. We then plot the distribution of coefficients and p-values. The results of this exercise are plotted in Figure A8. As can easily be observed, all coefficients are positive and substantively meaningful, centring around a median value of 0.071 (min = 0.046, max = 0.085), very similar to our main regression result. The corresponding p-values are tightly nestled against zero, with a median value of 0.003 (min = 0.0005, max= 0.056), indicating that our results do not depend on the specific combinations of controls.

Figure A8: Robustness to different combinations of control variables

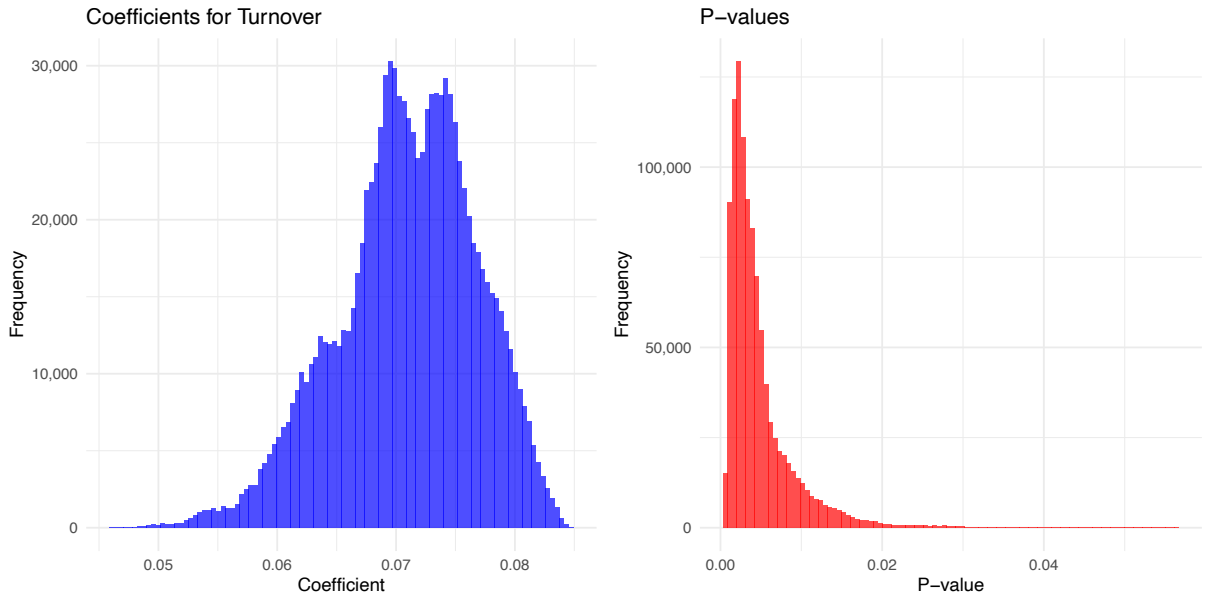

Note: Plots of coefficient size for our variable of focus, electoral turnover, and corresponding p-values for regressions using all possible combinations of control variables ($n = 2^{20} - 1 = 1,048,575$). Estimated using Equation 1 in the main text.

C.1.3 Bayesian Model Averaging

As some control variables such as age are particularly important predictors for excess mortality, we also consider Bayesian Model Averaging estimates of the turnover effect, as suggested in Montgomery and Nyhan (2010). Bayesian Model Averaging is similar in spirit to the investigation presented in section C.1.2 but differs in the weight given to each possible combination of control variables. In the previous section, any possible combination is given

equal weight, whereas Bayesian Model Averaging gives it a weight taking into account the prior probability for this combination and the amount of evidence for this combination in the data. More precisely, the posterior estimate for each combination is weighted by the posterior probability of this combination; in other words, each combination is weighted by its compatibility with the data. The Bayesian Model Averaged posterior distribution for any coefficient θ is given by:

$$P(\theta \mid \mathbf{y}) = \sum_{m=1}^{M} P(\theta \mid \mathbf{y}, M_m) P(M_m \mid \mathbf{y}) \tag{2}$$

where:

- θ is the coefficient of interest.
- $\mathbf{y}$ is observed data.
- M_m is the combination of control variables m out of M possible combinations.
- $P(\theta \mid \mathbf{y}, M_m)$is the posterior distribution of θ given the data $\mathbf{y}$ and for combination M_m.
- $P(M_m \mid \mathbf{y})$ is the posterior probability of combination M_m given the data $\mathbf{y}$.

In practice, we use the `BAS`(Clyde 2024) R package to efficiently explore the posterior distribution on all possible combinations. As we are interested in estimating the robustness to including certain control variables, we only consider combinations over the control variables, i.e. combination that include at least the intercept and the turnover variable. Figure A9 shows the space of combinations with the largest posterior probability. Some variables, such as the log proportion of the population over 80, appear consistently among the top combinations of control variables, while some, such as the log male-to-female ratio, are barely present. Figure A10 shows the posterior distribution on the turnover coefficient marginalised over all possible control variable combinations (Eq. 2). Coinciding with the conclusion at the beginning of the section, even considering uncertainty over all the possible combinations of control variables, the turnover effect is positive and very similar to the value estimated using only our selected combination. For illustration purposes, the figure also shows the posterior density (conditional on inclusion) on an unimportant variable, the log male-to-female ratio variable. It also includes the posterior probability of all the combinations where it is not included. The posterior probability of models where this variable is included is very small and even conditional on inclusion; the posterior distribution on the coefficient for this variable overlaps zeros.

C.1.4 R-square value at higher level of aggregation

One concern with our estimates may be that despite the large number of controls, our R-squared values tend to be low for all analyses. This is due to the extraordinarily difficult task of predicting mortality rates at the community level. At small levels of aggregation (such as the municipalities we work with), mortality events have a highly stochastic nature (Booth and Tickle 2008; Anson 2018). This problem becomes less pronounced at higher levels of aggregation, where mortality patterns tend to follow more predictable patterns. In turn,

Figure A9: Visualisation of the various control variables combinations with their posterior probability.

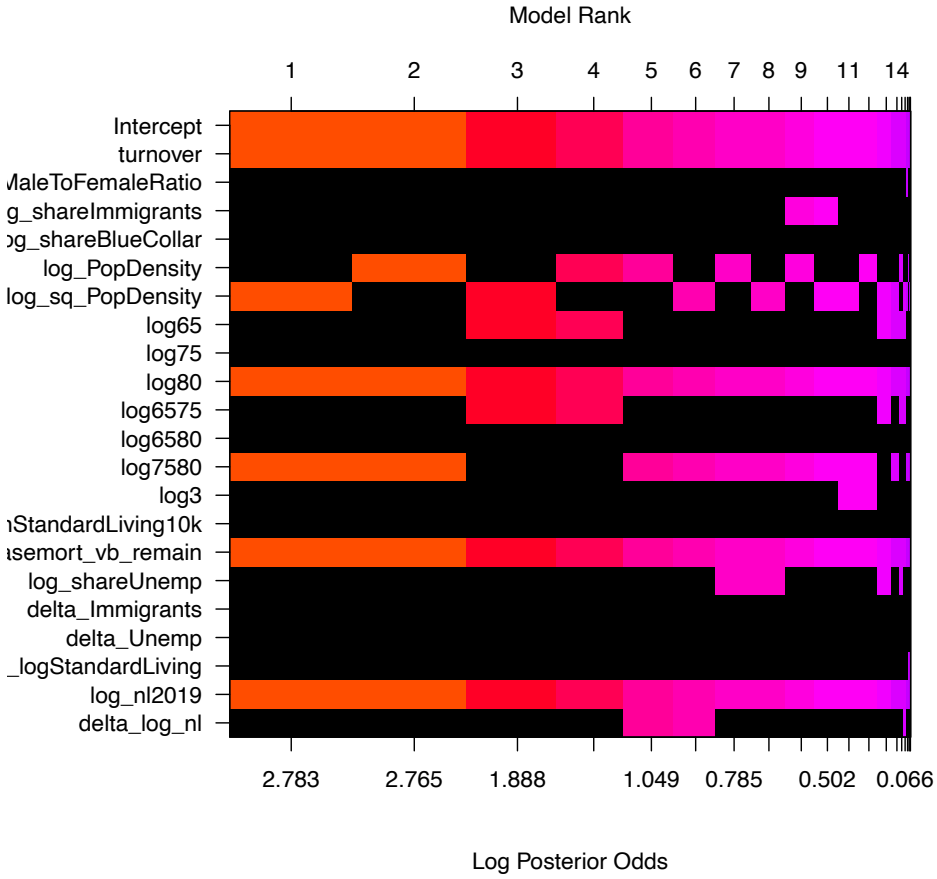

Note: Combinations of control variables are ranked according to their compatibility with the data, from most compatible to least compatible, from left to right. In each column, the variables not included in the model are displayed in black. In contrast, those included are highlighted with colours corresponding to their log posterior probability. The colour intensity of each column reflects the log of the posterior probabilities (displayed on the lower x-axis). These log posterior probabilities are scaled so that zero corresponds to the combination with the lowest probability among the top 20 combinations. Therefore, the axis values represent log Bayes factors comparing each model to the lowest probability combination in the top 20.

this means that models that predict a large fraction of the variation in mortality are easier to formulate at the aggregate level. Our case is no different, as we show in Table A17, where we present regression results for a specification where values are aggregated at the level of the 95 French *Département*. Note that in this specification, the independent variable is now the *share of municipalities that experienced a change of government*. In the bottom two rows, we therefore report the difference in the predictive margins of excess mortality when the turnover share is set to 0 compared to when it is set to 0.33 (the maximum value in the full sample).

Figure A10: Model averaged posterior distribution for two coefficients.

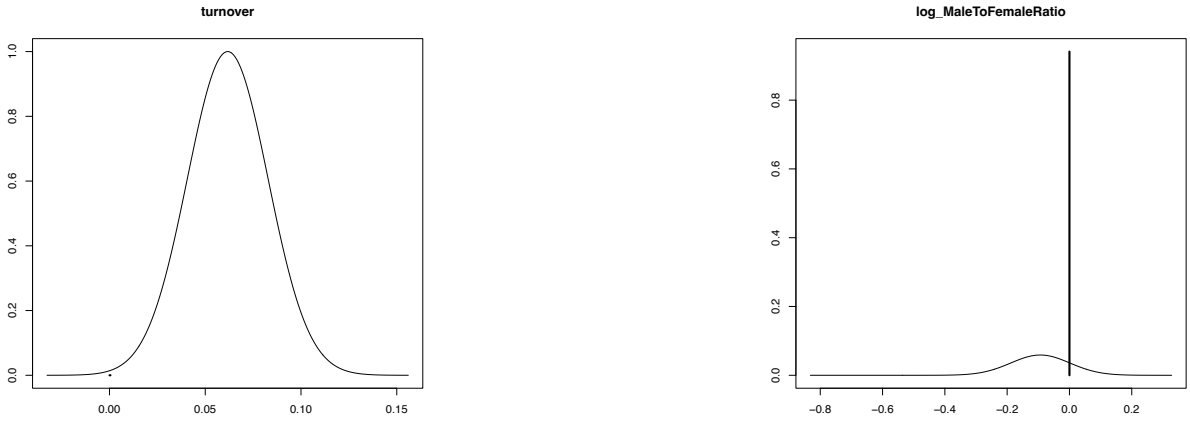

Note: Model averaged posterior distribution for the turnover coefficient and the log male to female ratio. The vertical bar represents the posterior probability that the effect is exactly zero (estimated from the posterior probability for the models without the covariates).

We can see that a) the share of municipalities with turnovers marginally predicts elevated levels of excess mortality even at this level (Model 1), b) that the size of the effect (0.096) is comparable to that estimated in the sample of municipalities, and that this effect is driven by left-leaning municipalities within *Départements* (Model 2), where the effects are statistically significant at conventional levels. Most importantly, we see that the R2 values are much higher than in the municipality analysis, ranging from 0.37 to 0.46, which gives us confidence that our low R-squares are due to the objective difficulty of predicting mortality for small areas rather than to problems with our specification.

Table A17: Association between share turnovers and excess mortality at Département level

	(1)	(2)	(3)
Share of municipalities that experienced electoral turnover	$0.298^{\dagger}$ (0.174)	$0.264^{\dagger}$ (0.147)	0.138 (0.173)
Pretreatment controls	Yes	Yes	Yes
N	95	95	94
R2	0.437	0.464	0.409
Diff in margins at share turnover [0.00,0.33]	0.098	0.087	0.046
P-value of difference	0.091	0.077	0.429

Note: Estimates for the effect of electoral turnovers on excess mortality with data aggregated at the level of the *Département*. Model 1: aggregate of all municipalities; Model 2: aggregate of left-leaning municipalities; Model 3: aggregate of center-/right-leaning muncipalities. OLS estimates, † $p < 0.1$, * $p < 0.05$, ** $p < 0.01$.

C.1.5 Direct regression

It is tempting to study the impact of turnovers on excess mortality by modelling death counts directly rather than using a two-step approach where excess mortality is estimated first and then examined in relation to turnover and control variables. However, the large number of municipalities puts this at the limit of the reach of classical inference methods. It would forbid the rich array of analyses and robustness checks that the two-step approach permits. The price to pay for the two-step approach is to discard the uncertainty in the estimates of the excess mortality factors, which is probably small for large municipalities but can be more prominent for small municipalities with a small number of deaths. Intuitively, ignoring uncertainty on the excess mortality factors likely overestimates their dispersion and could blur the signal to estimating the turnover effect. Therefore, as a robustness check, we also present an example of direct regression on the raw death counts to check if we observe a similar (and potentially stronger) turnover effect.

With notations similar to Section A.2, we consider the following model:

$$N_{i,y} \sim \text{Binomial}(\text{Pop}_{i,y}, \lambda_{i,y}) \tag{3}$$

$$\text{logit}\lambda_{i,y} = \alpha + \lambda_i + mort_i \delta_{\text{covid year}}(y) + \lambda_{\text{turnover}} \delta_{\text{covid year}}(y) X_{turnover,i} + \lambda_k X_{k,i} \tag{4}$$

$$\lambda_i \sim \mathcal{N}(0, \sigma) \tag{5}$$

$$mort_i \sim \mathcal{N}(0, \sigma_{\text{excess}}) \tag{6}$$

where again $N_{i,y}$ is the number of deaths observed in municipality i on the time period y (periods of 12 months starting from July 2015 to June 2019 and July 2020 to June 2021), $\text{Pop}_{i,y}$ is the population of municipality i during the time period y, λ_i is a random effect for the baseline mortality rate of municipality i pre-covid (period July 2015–June 2019), $mort_i$, appearing in Equation 1 is another random effect for the excess mortality factor during the Covid-19 pandemic, $\delta_{\text{covid year}}(y)$ is an indicator function which takes value 0 for the period pre-Covid and 1 for the period during the Covid-19 pandemic and $X_{turnover,i}$ is a binary variable equal to 1 if municipality i experienced a turnover in the 2020 municipal elections.

Equation 3 is a Binomial regression model with a logit link function, municipality random effects for the baseline mortality and the excess mortality, a fixed effect for the impact of the turnover during the Covid-19 period and the same controls as the main analysis (Eq. 1).

We fit this model using the R package `lme4` (Bates et al. 2015). As the optimisation is slightly challenging, we compare all optimisers available in R using the dedicated function `allFit`. In all cases, the turnover coefficient is consistently estimated at around 0.13 with a p-value $< 2e^{-16}$, which—via average predictive comparison over the municipalities which experienced a turnover (Gelman, Hill, and Vehtari 2020)—can be estimated as an extra 14 percentage points in the mortality, nearly double of what is estimated via linear regression. We also explored Bayesian mixed-effect binomial regression via the R package `rstanarm` (Goodrich et al. 2024; Brilleman et al. 2018), again resorting to Variational Inference, and obtained the same result. These results are in agreement with all our analyses and suggest that the two-step method used throughout the paper is a reasonable approach, which may at worst blur a little the effect of turnover on excess mortality.

C.2 Robustness of RD design

C.2.1 Density at cutoff of forcing variable

A central assumption of the regression discontinuity design is that there should be no sorting around the threshold. In other words, the forcing variable should be smoothly distributed across the threshold. We test for sorting effects around the threshold using the robust RD manipulation test suggested by Cattaneo, Jansson, and Ma (2020). The test fails to reject the null hypothesis that the density is continuous at the threshold. This is true both for the raw values (not controlling for any covariates, p=0.20) and even more clearly when the test is performed on the residualized values, removing the influence of the control variables as in the actual specification of the RD model (p=0.27). We visualize the density distribution of the incumbent's winning/losing margin in Figure A11. The margins look approximately normally distributed and, as suggested by the formal manipulation test, there is no visible clustering just before or just after the threshold.

Figure A11: Density distribution of forcing variable incumbent vote share

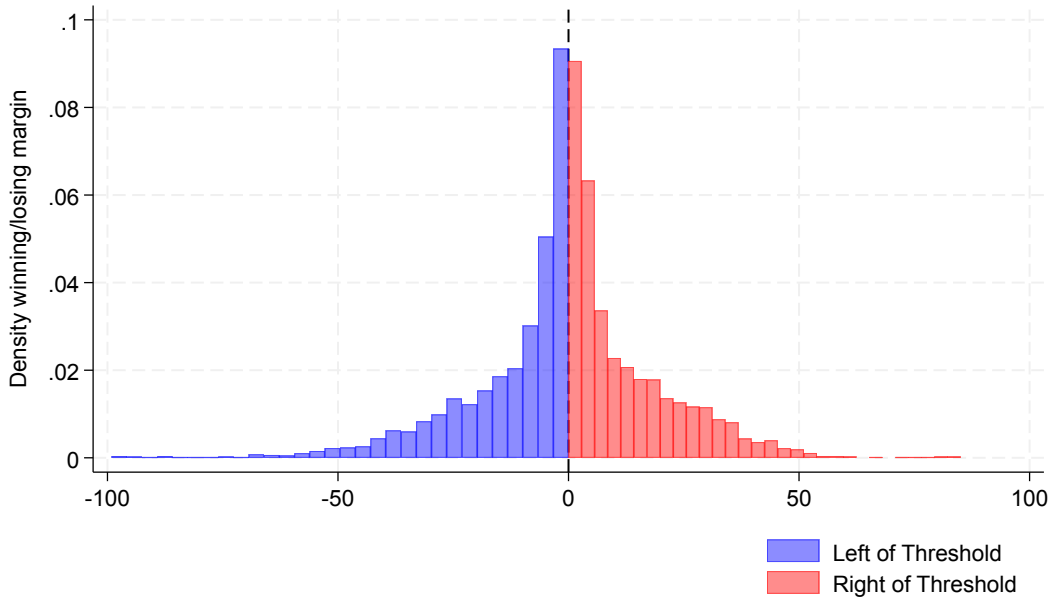

Note: Plot of density distributions for winning margins just above, and losing margins just below the threshold (zero).

C.2.2 Placebo tests using control variables

As a second robustness check, we run placebo tests using our control variables. We check for treatment effects of our forcing variable (incumbent winning/losing share), using each of the included control variables as the dependent variable. Since the control variables were collected before the elections, we should see no treatment effects—as long as the local randomization assumption holds, which implies that the covariates are similarly distributed at the threshold. As shown, this is indeed the case. Figure A12 shows the regression discontinuity plot for all control variables, and Table A18 provides point estimates (for the "robust" estimate following

Calonico, Cattaneo, and Titiunik (2014) and Calonico et al. (2019)), standard errors, and p-values. As can be seen, with the exception of the immigrant share (marginally significant at p=0.06), the values for the control variables are all statistically indistinguishable just before and just after the threshold.

Table A18: Coefficient estimates for placebo tests

Dependent variable	RD coefficient (1)	SE (2)	p-value (3)
Male/female ratio	0.002	0.010	0.85
Share over 65	0.004	0.003	0.13
Share over 75	-0.001	0.001	0.43
Share over 80	0.000	0.001	0.77
Share blue collar	0.002	0.004	0.61
Median standard of living	0.002	0.008	0.78
Population density	0.055	0.122	0.65
Baseline mortality	0.000	0.001	0.77
Unemployment rate	0.001	0.002	0.59
Share immigrants	-0.010†	0.005	0.06
Nightlight emissions 2019	0.011	0.112	0.92
Change in nightlight emissions	-0.057	0.046	0.21
Change in share immigrants	0.002	0.002	0.20
Change in unemployment	-0.001	0.001	0.69
Change in standard of living	-0.003	0.067	0.97

Note: RD coefficient estimates for control variables, 'robust' regression discontinuity estimates following Calonico, Cattaneo, and Titiunik (2014) and Calonico et al. (2019). The forcing variable is that incumbent vote share 2020; † $p < 0.1$, * $p < 0.05$, ** $p < 0.01$.

Figure A12: RD placebo tests with control variables

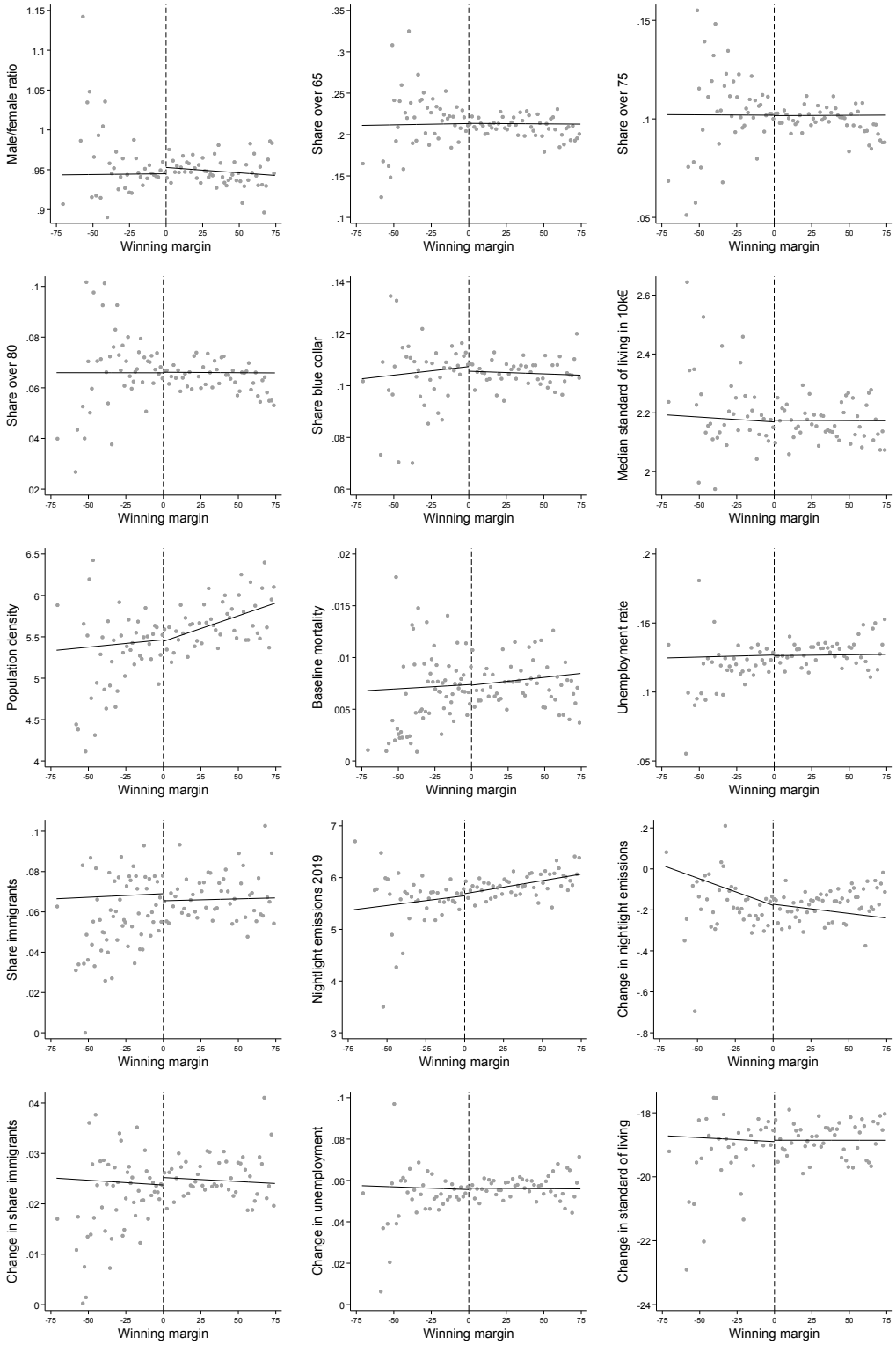

D Country-level panel dataset

Figure A13: Trends in excess mortality in democracies vs. flawed democracies and autocracies

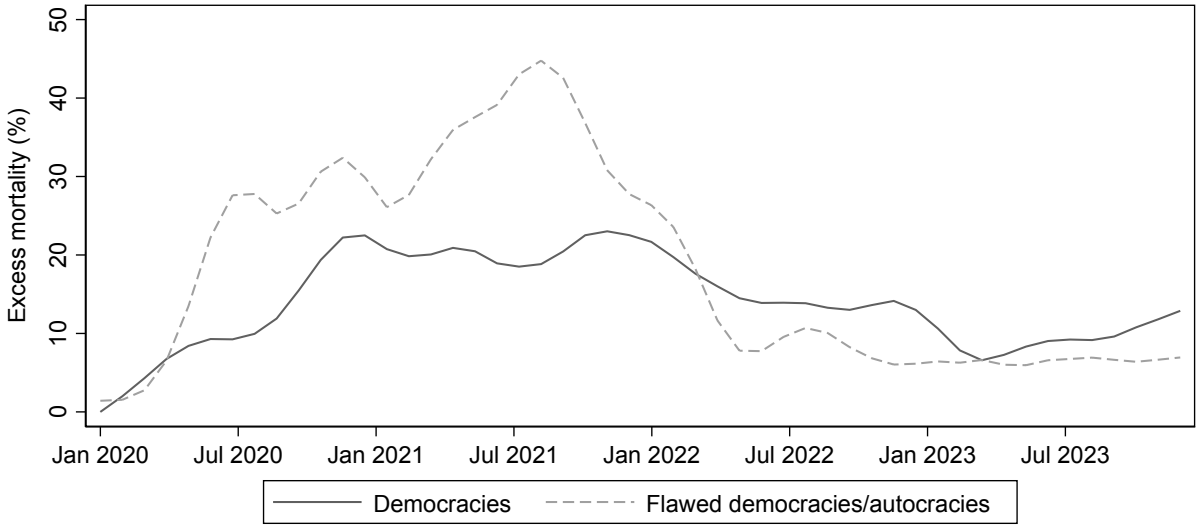

Note: Trends in excess mortality (in %) in democracies vs. flawed democracies and autocracies between 2020 and 2023. Democracies are defined as scoring 0.6 or higher on the V-Dem liberal democracy index. Countries and territories classified as democracies: Argentina, Armenia, Australia, Austria, Barbados, Belgium, Canada, Cape Verde, Chile, Costa Rica, Croatia, Cyprus, Czechia, Denmark, Estonia, Finland, France, Germany, Greece, Iceland, Ireland, Israel, Italy, Jamaica, Japan, Latvia, Lithuania, Luxembourg, Netherlands, New Zealand, Norway, Peru, Portugal, Slovakia, Slovenia, South Africa, South Korea, Spain, Sweden, Switzerland, Taiwan, Tunisia, United Kingdom, United States, Uruguay. Countries and territories classified as flawed democracies or autocracies: Albania, Algeria, Azerbaijan, Belarus, Bhutan, Bolivia, Bosnia & Herzegovina, Brazil, Bulgaria, Colombia, Cuba, Dominican Republic, Ecuador, Egypt, El Salvador, Georgia, Guatemala, Hungary, Iran, Jordan, Kazakhstan, Kosovo, Kuwait, Kyrgyzstan, Lebanon, Malaysia, Maldives, Malta, Mauritius, Mexico, Moldova, Mongolia, Montenegro, Namibia, Nicaragua, North Macedonia, Oman, Palestinian Territories, Panama, Paraguay, Philippines, Poland, Qatar, Romania, Russia, Serbia, Seychelles, Singapore, Suriname, Tajikistan, Thailand, Turkey, Ukraine, United Arab Emirates, Uzbekistan.

Figure A14: Effect (DiD) of electoral turnovers in democracies and non-democracies

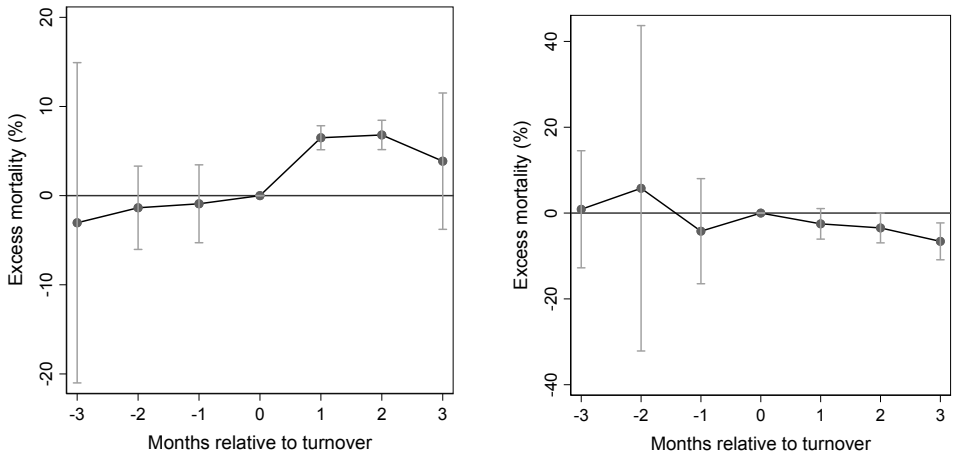

(a) Democracies (b) Flawed democracies/autocracies

Note: DiD/panel event study plot following De Chaisemartin and D'Haultfœuille (2024) comparing effects of electoral turnovers on excess mortality in democracies vs. flawed democracies and autocracies. Markers are point estimates, lines are 95 percent confidence intervals.

Table A19: Countries and territories by democracy and turnover (2020–2023) status

Democracies with turnover	**Democracies without turnover**
Argentina, Austria, Barbados, Belgium, Canada, Cape Verde, Denmark, Estonia, France, Hong Kong, Iceland, Jamaica, Japan, Latvia, Luxembourg, Mauritius, Namibia, Netherlands, Palestine, Panama, Portugal, Spain, Switzerland, Taiwan, United Kingdom, Uruguay	Australia, Brazil, Bulgaria, Chile, Costa Rica, Croatia, Cyprus, Czechia, Finland, Germany, Greece, Ireland, Italy, Kosovo, Lithuania, New Zealand, Norway, Peru, Poland, Slovakia, Slovenia, South Korea, Suriname, Sweden, Tunisia, United States
Flawed democracies/autocracies with turnover	**Flawed democracies/autocracies without turnover**
Bolivia, Colombia, Dominican Republic, Ecuador, Israel, Malaysia, Moldova, Montenegro, Paraguay, Romania, Seychelles, Singapore, Thailand	Albania, Algeria, Armenia, Azerbaijan, Belarus, Bhutan, Bosnia and Herzegovina, Cuba, Egypt, El Salvador, Georgia, Guatemala, Hungary, Iran, Jordan, Kazakhstan, Kuwait, Kyrgyzstan, Lebanon, Maldives, Malta, Mexico, Mongolia, Nicaragua, North Macedonia, Oman, Philippines, Qatar, Russia, Serbia, South Africa, Tajikistan, Turkey, Ukraine, United Arab Emirates, Uzbekistan

Note: List of countries and territories depending on whether they can be classified as democracies (0.6 on V-Dem's liberal democracy index 2019) and on whether they experienced an electoral turnover between 2020 and 2023.

References

Anson, Jon. 2018. "Estimating Local Mortality Tables for Small Areas: An Application Using Belgian Sub-Arrondissements." *Quetelet Journal* 6, no. 1 (1 2018): 73–97.

Banerjee, Abhijit V, and Esther Duflo. 2011. *Poor Economics: A Radical Rethinking of the Way to Fight Global Poverty.* New York: PublicAffairs.

Bates, Douglas, Martin Mächler, Ben Bolker, and Steve Walker. 2015. "Fitting Linear Mixed-Effects Models Using lme4." *Journal of Statistical Software* 67 (1): 1–48.

Blei, David M, Alp Kucukelbir, and Jon D McAuliffe. 2017. "Variational Inference: A Review for Statisticians." *Journal of the American Statistical Association,* no. just-accepted.

Booth, H., and L. Tickle. 2008. "Mortality Modelling and Forecasting: A Review of Methods." *Annals of Actuarial Science* 3, nos. 1-2 (September): 3–43.

Brilleman, SL, MJ Crowther, M Moreno-Betancur, J Buros Novik, and R Wolfe. 2018. *Joint longitudinal and time-to-event models via Stan.* StanCon 2018. 10-12 Jan 2018. Pacific Grove, CA, USA.

Calonico, Sebastian, Matias D. Cattaneo, Max H. Farrell, and Rocío Titiunik. 2019. "Regression Discontinuity Designs Using Covariates." *The Review of Economics and Statistics* 101, no. 3 (July 1, 2019): 442–451.

Calonico, Sebastian, Matias D. Cattaneo, and Rocio Titiunik. 2014. "Robust Nonparametric Confidence Intervals for Regression-Discontinuity Designs." *Econometrica* 82 (6): 2295–2326.

Campbell, Angus, Philip E. Converse, Warren E. Miller, and Donald E. Stokes. 1960. *The American Voter.* Chicago, IL: University of Chicago Press.

Cattaneo, Matias D., Michael Jansson, and Xinwei Ma. 2020. "Simple Local Polynomial Density Estimators." *Journal of the American Statistical Association* 115, no. 531 (July 2, 2020): 1449–1455.

Clyde, Merlise. 2024. *BAS: Bayesian Variable Selection and Model Averaging using Bayesian Adaptive Sampling.* R package version 1.7.5.

De Chaisemartin, Clément, and Xavier D'Haultfœuille. 2024. "Difference-in-Differences Estimators of Intertemporal Treatment Effects." *The Review of Economics and Statistics* (February 9, 2024): 1–45.

Elvidge, Christopher D., Kimberly E. Baugh, Eric A. Kihn, Herbert W. Kroehl, and Ethan R. Davis. 1997. "Mapping City Lights with Nighttime Data from the DMSP Operational Linescan System." *Photogrammetric Engineering and Remote Sensing* 63 (6): 727–734.

Elvidge, Christopher D., Mikhail Zhizhin, Tilottama Ghosh, Feng-Chi Hsu, and Jay Taneja. 2021. "Annual Time Series of Global VIIRS Nighttime Lights Derived from Monthly Averages: 2012 to 2019." *Remote Sensing* 13, no. 5 (5): 922.

Elwert, Felix. 2014. "Graphical Causal Models." In *Handbook of Causal Analysis for Social Research,* edited by Stephen L Morgan, 245–273. Dordrecht: Springer.

Gelman, Andrew, Jennifer Hill, and Aki Vehtari. 2020. *Regression and Other Stories.* Cambridge University Press.

Ghosh, Tilottama, Kimberly E. Baugh, Christopher D. Elvidge, Mikhail Zhizhin, Alexey Poyda, and Feng-Chi Hsu. 2021. "Extending the DMSP Nighttime Lights Time Series beyond 2013." *Remote Sensing* 13, no. 24 (24): 5004.

Goodrich, Ben, Jonah Gabry, Imad Ali, and Sam Brilleman. 2024. *rstanarm: Bayesian applied regression modeling via Stan.* R package version 2.32.1.

Kucukelbir, Alp, Rajesh Ranganath, Andrew Gelman, and David M Blei. 2015. "Automatic Variational Inference in Stan." *arXiv preprint arXiv:1506.03431.*

Le Monde. 2020. "Municipales 2020: entre LRM et la droite, le rapprochement perpétuel," June 8, 2020.

Montgomery, Jacob M., and Brendan Nyhan. 2010. "Bayesian Model Averaging: Theoretical Developments and Practical Applications." *Political Analysis* 18, no. 2 (April): 245–270.

Noury, Abdul, Abel François, Olivier Gergaud, and Alexandre Garel. 2021. "How Does COVID-19 Affect Electoral Participation? Evidence from the French Municipal Elections." *PLOS ONE* 16, no. 2 (February 24, 2021): e0247026.

Oster, Emily. 2019. "Unobservable Selection and Coefficient Stability: Theory and Evidence." *Journal of Business & Economic Statistics* 37, no. 2 (April 3, 2019): 187–204.

Patel, J.A., F.B.H. Nielsen, A.A. Badiani, S. Assi, V.A. Unadkat, B. Patel, R. Ravindrane, and H. Wardle. 2020. "Poverty, Inequality and COVID-19: The Forgotten Vulnerable." *Public Health* 183 (June): 110–111.

Petrilli, Christopher M., Simon A. Jones, Jie Yang, Harish Rajagopalan, Luke O'Donnell, Yelena Chernyak, Katie A. Tobin, Robert J. Cerfolio, Fritz Francois, and Leora I. Horwitz. 2020. "Factors Associated with Hospital Admission and Critical Illness among 5279 People with Coronavirus Disease 2019 in New York City: Prospective Cohort Study." *BMJ* 369 (May 22, 2020): m1966.

Pryor, Laura, Katrine Strandberg-Larsen, Anne-Marie Nybo Andersen, Naja Hulvej Rod, and Maria Melchior. 2019. "Trajectories of Family Poverty and Children's Mental Health: Results from the Danish National Birth Cohort." *Social Science & Medicine* 220 (January 1, 2019): 371–378.

Schaub, Max. 2021. "Acute Financial Hardship and Voter Turnout: Theory and Evidence from the Sequence of Bank Working Days." *American Political Science Review* 115, no. 4 (November): 1258–1274.

Stan Development Team and Stan Developement Team. 2015. "Stan: A C++ Library for Probability and Sampling, Version 2.7.0."

Wagstaff, Adam. 2002. "Poverty and Health Sector Inequalities." *Bulletin of the World Health Organization* 80:97–105.

Williamson, Elizabeth J., Alex J. Walker, Krishnan Bhaskaran, Seb Bacon, Chris Bates, Caroline E. Morton, Helen J. Curtis, et al. 2020. "Factors Associated with COVID-19-related Death Using OpenSAFELY." *Nature* 584, no. 7821 (7821): 430–436.